CONF-931087--2

Experimental Analysis of Natural Convection Within a Thermosyphon

RECEIVED
SEP 27 1993
OSTI

Randy Clarksean
Fuel Cycle Division
Argonne National Laboratory
P.O. Box 2528
Idaho Falls, Idaho 83403

Abstract

The heat transfer characteristics of a thermosyphon designed to passively cool cylindrical heat sources are experimentally studied. The analysis is based on recognizing the physics of the flow within different regions of the thermosyphon to develop empirical heat transfer correlations. The basic system consists of three concentric cylinders, with an outer channel between the outer two cylinders, and an inner channel between the inner two cylinders. Tests were conducted with two different process material container diameters, representing the inner cylinder, and several different power levels. The experimentally determined local and average Nu numbers for the inner channel are in good agreement with previous work for natural convection between vertical parallel plates, one uniformly heated and the other thermally insulated. The implication is that the heat transfer off of each surface is independent of the adjacent surface for sufficiently high Ra numbers. The heat transfer is independent because of limited interaction between the boundary layers at sufficiently high Ra numbers. As a result of the limited interaction, the maximum temperature within the system remained constant, or decreased slightly when the radii of the inner cylinders increased for the same amount of heat removal.

1 Introduction

The use of thermosyphons are important in a variety of applications. The applications include the cooling of electronic components ([1]), heat removal systems for nuclear reactors ([2] and [3]), solar energy systems ([4]), and other industrial applications. The use of passive systems, or thermosyphons, has increased because they are less expensive than forced cooling systems, and because they do not require blowers or pumps for fluid circulation. In addition, the systems are more dependable because they operate without any external control signals or power, which insures they will continue to function under all operating conditions.

The submitted manuscript has been authored by a contractor of the U.S. Government under contract no. W-31-109-ENG-38. Accordingly, the U.S. Government retains a non-exclusive, royalty-free license to publish or reproduce the published form of this contribution, or allow others to do so, for U.S. Government purposes.

The current analysis is for a system to passively cool process materials from the Integral Fast Reactor Fuel Cycle Facility. The process materials are part of a pyrometallurgical process for reprocessing spent metallic fuel from Experimental Breeder Reactor II (EBR-II). The process materials will temporarily be stored in cylindrical pits within the floor of the Fuel Cycle Facility. A full discussion of the Integral Fast Reactor concept can be found in [5].

A thermosyphon uses natural convection to generate flow within the system. For the system under consideration here, there are two basic phenomenon. The inner channel is clearly dominated by a natural convection phenomena. The flow within the outer channel is a combination of forced and free convection. The "forced" convection flow component is the result of the fluid being drawn through this channel by the buoyancy forces in the inner channel. The forced flow is opposed by the buoyant forces generated on the outer surface of the chimney.

A variety of work has been conducted on different types of thermosyphons. General reviews of thermosyphons can be found in References [6] and [7].

For the present configuration, work related to natural convection off of vertical cylinders, vertical plates, and between vertical parallel plates is of interest. These configurations represent the basic mechanisms related to natural and mixed convection in the system (see [8] to [9]). The development of flow between vertical parallel plates has been numerically analyzed in [11] and [12].

Reference [10] analyzed the effect of surface curvature and Pr number for laminar natural convection along vertical cylinders. As the curvature of the surface increased for a given Pr number, the local heat transfer coefficient increased. As the surface curvature increased, the ratio of the local Nu number for a cylinder to that of a flat plate increased, up to 10 to 20 times greater in some instances.

The intent of this paper is to determine the local Nu numbers within a thermosyphon. The correlations of the Nu numbers will be based on the physics

Presented at the 3rd World Conference on Experimental Heat Transfer, Fluid Mechanics and Thermodynamics, Honolulu, Hawaii, USA, October 31 - November 5, 1993

MASTER

DISTRIBUTION OF THIS DOCUMENT IS UNLIMITED

DISCLAIMER

This report was prepared as an account of work sponsored by an agency of the United States Government. Neither the United States Government nor any agency thereof, nor any of their employees, makes any warranty, express or implied, or assumes any legal liability or responsibility for the accuracy, completeness, or usefulness of any information, apparatus, product, or process disclosed, or represents that its use would not infringe privately owned rights. Reference herein to any specific commercial product, process, or service by trade name, trademark, manufacturer, or otherwise does not necessarily constitute or imply its endorsement, recommendation, or favoring by the United States Government or any agency thereof. The views and opinions of authors expressed herein do not necessarily state or reflect those of the United States Government or any agency thereof.

of the flow near each surface. Comparisons of the Local Nu numbers with previously conducted numerical and experimental work for vertical parallel plates will also be made. Overall, the paper will present an approach based on analyzing the physics of the flow which could be applied to other thermosyphons. The remainder of the paper will address the experimental apparatus, the data reduction techniques, and a discussion of the results.

2 Experimental Apparatus

The experimental apparatus was a full scale simulation of the actual pits. Air was used as the working fluid in the experiment. A schematic of the system is found in Figure 1.

The heat source is located within the process material containers (waste cans). The containers, "chimney," and the pipeliner are all cylindrical. Two different container sizes were used for the tests. One container was 18.8 cm (4.25 inches) in diameter, and 74.9 cm (29.5 inches) long. Three of these containers, which will be referred to as small cans, were stacked and made up the inner cylinder for one group of tests. The second container was 16.8 cm (6.625 inches) in diameter, and 141 cm (55.5 inches) long. Two of theses containers, which will be referred to as the large cans, were stacked and used for the second set of tests. Each of the containers consist of an electrical heater surrounded by copper shot. The heater is nearly the full length of the container and is located at the center of the container. The heater simulates the heat generating characteristics of the process materials.

The flow channels are narrow compared to their length. The outer channel width is 3.18 cm (1.25 inches). The inner channel width is either 4.96 cm (1.95 inches) or 2.26 cm (0.89 inches), for the small cans and the large cans respectively. The total length of each channel is approximately 300 cm (118 inches).

The "chimney" is an insulated pipe to minimize the heat transfer from the containers to the inlet flow stream. The chimney consists of a thin-walled pipe, 1.27 cm (0.5 inch) of fiber insulation, and a thin layer of stainless steel on the outside to protect the insulation. Insulation was placed on the outer surface of the pipeliner to represent the concrete surrounding the pipes.

The operating temperature of the containers ranges from 30 to 325°C. In this operating range, radiative and convective heat transfer mechanisms will be important for heat removal from the containers. Energy is radiated from the waste cans to the inner surface of the chimney. Once the energy reaches this surface, it is either convected off the surface, or conducted through the chimney to the outer channel. The energy which conducts through the chimney is then convected away by the flow entering the system in the outer channel. For the high temeprature tests, approximately 60 percent of the energy was convected off of the waste cans. The remaining 40 percent of the energy was radiated to the inner chimney surface. This energy was then convected off the inner and outer chimney surfaces.

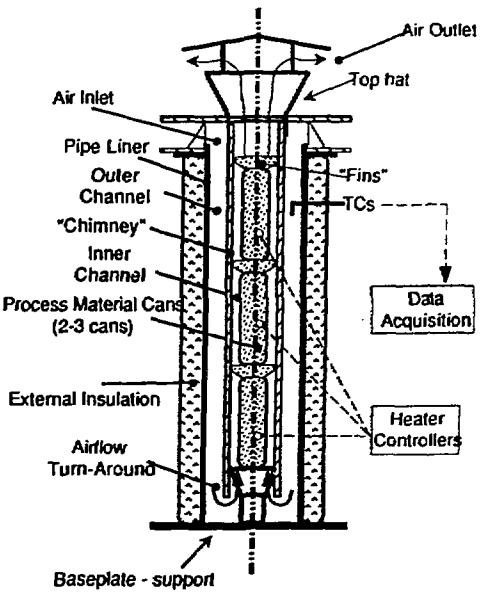

Figure 1: Schematic of Experimental Apparatus.

Buoyant forces are generated along the inner chimney and waste container surfaces. These buoyancy forces draw fluid down the outer channel, into the inner channel, and out the top of the apparatus. The environment outside of the pit is maintained at nearly a constant temperature. The system operates as a thermosyphon, or more specifically, as a free convection fluid loop with a constant temperature reservoir (see [7]).

The top of each container has a finned attachment for centering the containers within the chimney. The finned region above each container causes a recirculation zone to form as the flow comes off of the container.

Approximately 120 thermocouples were used to measure surface temperatures of the containers, chimney, and the pipeliner. Thermocouples were also used to measure the temperature profile of the air within the channels, the inlet air temperature, and

the outlet air temperature. All of the thermocouples were of type K. The thermocouples were spot welded onto the surfaces of the waste cans, the inner and outer chimney surfaces, and the pipeliner. A Keithley-Metrabyte data acquisition system and a personal computer were used to record the data. Temperature measurements were accurate within ± 1.2°C.

Preliminary testing was conducted with the thermocouple arrays to measure the temperature profile of the air in the channels. In general, the thermocouple arrays were capable of measuring the fluid temperature, but not the fluid temperature in regions of large temperature gradients near the walls. The only thermocouple array which was used for data reduction was the array at the bottom end of the outer channel. The fluid temperatures across the channel in this region were nearly uniform.

The velocity profile above the top can was measured by a velocity probe and will be used for qualitative discussions only. The velocity measurements are qualitative because the probe requires the flow to be fully-developed, and the distance to the probe did not allow for fully developed flow. The power input to the containers was individually controlled and measured. The calculated power measurements were within ±3 to ±8 percent.

3 Data Reduction

The analysis of the data relied on surface temperatures and calculation procedures. The transfer of energy off of the surfaces in the inner channel is clearly driven by buoyancy. The transfer of energy in the outer channel will depend on the flow rate and buoyancy forces generated on each of the surfaces. The importance of each effect can be determined by analyzing the data for mixed convection effects.

The mass flow rate through the system was determined from the total energy released and the temperature rise of the fluid.

$$\dot{m} = \frac{Q_{total}}{C_p(T_{inlet} - T_{outlet})} \tag{1}$$

The outlet temperature, T_{outlet}, was calculated by using measured temperatures of the flow across the outlet of the experiment. A slug flow profile was assumed. Using worst case assumptions for the outlet flow profile, the uncertainty of $\dot{m}$ ranged between ±10 and ±16 percent.

The flow through the system can be represented by a Re number for the flow in either the inner or outer channel, where

$$Re = \frac{\rho V D_h}{\mu} = \frac{\dot{m} D_h}{\mu A} \tag{2}$$

The total flux of energy at a point on a surface can be defined as

$$q''_{tot} = q''_{rad} + q''_{cond} + q''_{loc} \tag{3}$$

The local, or convective heat flux, q''_{loc}, is the required data for the calculation of the local Nu, Ra, and mixed convection parameters. The radiative fluxes were calculated between the inner and outer surfaces of each channel. The measured temperatures and the best estimates of the surface emissivities were used in making these calculations. The emissivities for the waste cans and chimney surfaces were 0.8 and 0.3 respectively.

For the surface of the waste cans, the total flux equals the radiative and convective fluxes off the surface. The total flux at the surface of the waste can was assumed to be a constant.

The calculation of the convective flux off of the inner surface of the chimney was more complicated. On the inner surface of the chimney, the heat balance consists of radiative, convective, and conductive components. Conduction must be considered because some of the energy is transported through the chimney to the outer surface of the chimney. The conductive fluxes for the inner and outer surfaces of the chimney were calculated by using a two-dimensional cylindrical conduction model and the measured surface temperatures.

Once the local heat fluxes were determined, the local Nu and Ra numbers could be obtained. The local Nu and Ra numbers are defined as shown below:

$$Nu_{loc} = \frac{h_{loc}\Delta r}{k} = \frac{q''_{loc}\Delta r}{(T_w - T_{bf\ ref})k} \tag{4}$$

$$Ra_{loc} = \frac{q''_{loc}\Delta r^4 \beta\, g}{\alpha \nu k} \tag{5}$$

The uncertainty of Nu_{loc} ranged between ±10 and ±15 percent. The uncertainty of Ra_{loc} was estimated to be ±20 percent.

The reference temperature, $T_{bf\ ref}$, was selected to represent the free stream temperature available for the development of the boundary layer. For the outer channel, the reference temperature was the inlet temperature, T_o. The bulk fluid temperature at the bottom of the outer channel was used as the reference temperature for the inner surface of the chimney, and for the surface of the first waste can. This is a reasonable estimate because the fluid will be well mixed in the lower regions of the apparatus before

entering the inner channel.

At the top of each waste can, there is a set of fins to center the can in the chimney. The fins allow a recirculation zone to form, which can assist in mixing the fluid coming off the can and allow for the development of a new boundary layer on the can above. The bulk fluid temperature at this location was used for the calculation of the local Nu numbers for the can surface above the finned region. $T_{bf\ ref}$ was calculated knowing the total amount of energy added to the flow upstream of the given location.

A different form of the Ra number has typically been used for correlating data for vertical parallel plates, and will be used here (see [13] and [14]). The modified form of the local Ra number is

$$Ra_{loc}\frac{\Delta r}{x(i)} = \frac{q''_{loc}\Delta r^4 \beta\ g}{\alpha\nu k}\frac{\Delta r}{x(i)} \qquad (6)$$

For the surfaces in the outer channel, $x(i)$ was taken as the distance from the inlet. For the inner chimney surface, $x(i)$ was taken as the distance from the bottom of the channel. For the waste cans, $x(i)$ was taken as the distance from the bottom of each can. The bottom of each can was used because it represents of the start of the boundary layer on each can. The fluid properties for the local Nu and Ra numbers were evaluated at the average of the wall and reference temperatures.

The heat transfer in the outer channel was analyzed to determine if mixed convection effects were significant. Mixed convection best represents the mechanism for heat removal from these surfaces. As the effect of buoyancy opposing the flow increases, the overall heat transfer may be increased or decreased, relative to what would occur for only forced convection. Reference [15] suggests the following parameters be used when analyzing for mixed convection effects for a $Pr < 1$.

$$\frac{Nu_x}{Re_x^{\frac{1}{2}}Pr^{\frac{1}{3}}} \quad , \quad \frac{Bo_x^{\frac{1}{4}}}{Pe_x^{\frac{1}{2}}}$$

In general, for a $Pr < 1$, natural convection and forced convection dominate for the following regimes

$$\frac{Bo_x^{\frac{1}{4}}}{Pe_x^{\frac{1}{2}}} \begin{cases} > O(1), \text{ Natural Convection} \\ < O(1), \text{ Forced Convection} \end{cases} \qquad (7)$$

4 Discussion of Results

Two sets of tests were conducted, one with three stacked small cans, and one with two stacked large cans. The majority of the tests were conducted with each of the containers generating an equal amount of energy. A few tests were conducted for a different energy generation in each can.

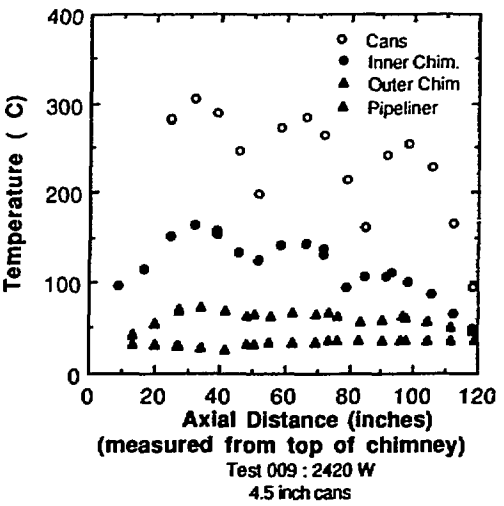

Figure 2: Surface Temperature Profile.

Figure 2 shows a representative axial temperature profile. The temperature profile is for a test conducted with the small cans. The temperatures for each of the surfaces are shown. The surfaces include the waste can surfaces, the inner and outer surfaces of the chimney, and the surface of the pipeliner. The axial distance is measured from the top to the bottom of the chimney.

The temperature profiles of the containers are affected by the fins. The three containers are clearly identified by the drop in temperature for the tops and bottoms of the cans. The drop in temperature results from the breakdown of the boundary layer as the flow recirculates at the top of each can and starts developing on the can above, the convective loss of energy from the surface of the fins, and the conduction of the energy from the containers to the chimney through the fins.

During some of the tests, the flow within the system was oscillatory. Figure 3 shows the velocity data at the outlet of the experiment for one sample point. Velocity measurements at other sample points also showed similar trends for this particular test. At higher average Ra numbers, the flow within the system was steady, and not oscillatory.

Figure 4 shows the results of the data reduction for the waste can surfaces. The local Nu number is plotted versus the modified local Ra number defined in Equation 6. There are two curves which represent

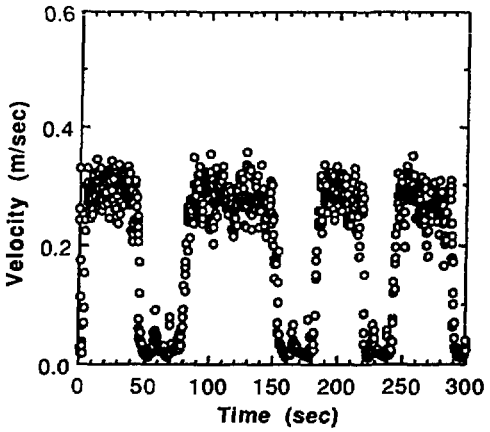

Figure 3: Oscillatory velocity profile at one sample location at the outlet of the experiment.

the data for the large can tests (smaller gap width) and the small can tests (larger gap width).

There are some points that clearly lie outside the majority of the data. The highest Ra number data for the small can tests are more erratic because of the additional surface area exposed to the flow on the bottom of the cans. A similar effect is found at the top of each waste can. The recirculation at the top of each can also results in an increased heat transfer area. The increased surface area causes T_w to be decreased, which results in higher than expected Nu numbers.

Figure 5 shows a comparison of the local Nu numbers between the current experimental data and the numerical work of [13]. Reference [13] experimentally and numerically studied natural convection between vertical parallel plates. One of the plates had a uniform flux, and the other plate was thermally insulated. The numerical predictions are for the local Nu numbers versus the local modified Ra number $Ra\frac{\Delta r}{x(i)}$. The average Ra numbers for the two sets of numerical data are 800 and 2600. The average Ra numbers for the surface of the large waste cans fall into this range. In general, there is excellent agreement between the numerical results for parallel plates and the waste can surface. The experimental results are slightly higher, but the average Nu numbers should be higher for a curved surface. This effect is pointed out for natural convection by [10], and for forced convection by [17].

The results for the local Nu from the inner chimney surface are shown in Figure 6.The two relationships are for the small diameter can and the large diameter can. Figure 6 highlights some of the scattered data points. The inlet to the inner channel shows a sensitivity to the selection of T_{bf}. The outlet of the inner channel also shows an offset from the other data. Heat losses from the top of the experiment can account for this offset.

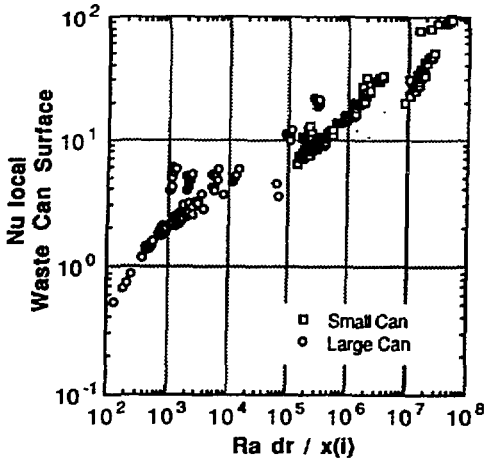

Figure 4: Nu_{loc} vs. Ra_{loc} for the waste can surfaces.

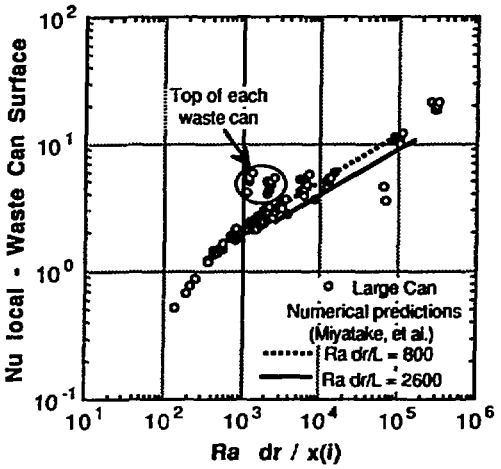

Figure 5: A comparison between the current experimental data for the inner chimney surface and the numerical work of Miyatake, et al.

The local heat transfer data for the outer channel is shown in Figure 7. The data is presented in terms of the nondimensional parameters discussed in the data reduction section. In general, the $\frac{Nu}{Re^{\frac{1}{2}}Pr^{\frac{1}{3}}}$ values approach a constant for low values of $\frac{Bo^{\frac{1}{4}}}{Pe^{\frac{1}{2}}}$. The leveling out of the data indicates the heat transfer approaches the forced convection limit. As $\frac{Nu}{Re^{\frac{1}{2}}Pr^{\frac{1}{3}}}$ increases, the effects of natural convection become more important. The indications are that the flow is in the mixed convection regime and that buoyancy

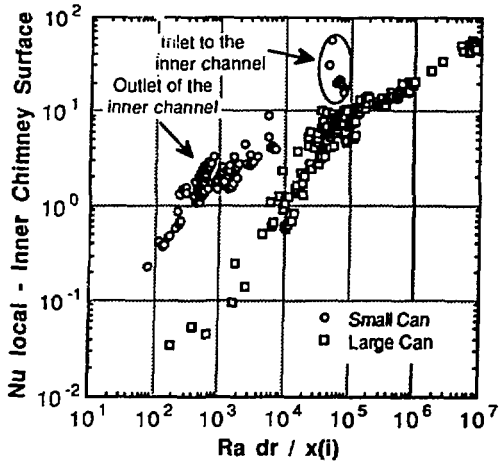

Figure 6: Local Nu number results for the inner chimney surface.

must be considered.

The average Nu number data for the inner channel are presented in Figure 8. The data correlates very well for the waste can (smaller radii) and the inner chimney surfaces (larger radii). The data spans over two orders of magnitudes for the average Ra number, and over an order of magnitude for the average Nu number. The curve fits for the waste can and inner chimney surfaces are respectively

$$Nu_{avg-wc} = 0.556\left(Ra\frac{\Delta r}{L}\right)^{0.29}_{avg}$$

$$Nu_{avg-ic} = 0.453\left(Ra\frac{\Delta r}{L}\right)^{0.27}_{avg}$$

Figure 8 also shows a comparison with the experimentally obtained average Nu number data from [18]. Nu number data from [18] is for heat transfer between vertical parallel plates, one surface heated, the other surface insulated. In general, there is good agreement between the trends shown for the parallel plate data and the present experiment. As mentioned previously, surface curvature causes an increase in the average Nu numbers.

The mass flow through the system can be addressed by correlating the Re number with the average Ra number for the waste can surface. The average Re number data collapsed to one relationship when the ratio of the cross- sectional flow areas for the inner and outer channels were considered as shown in Figure 9. The area ratio represents the amount of resistance to the flow present in the outer channel relative to the inner channel. The use of the

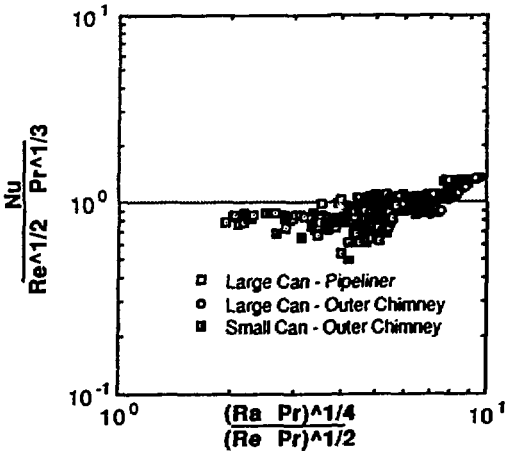

Figure 7: The mixed convection local heat transfer data for the outer channel.

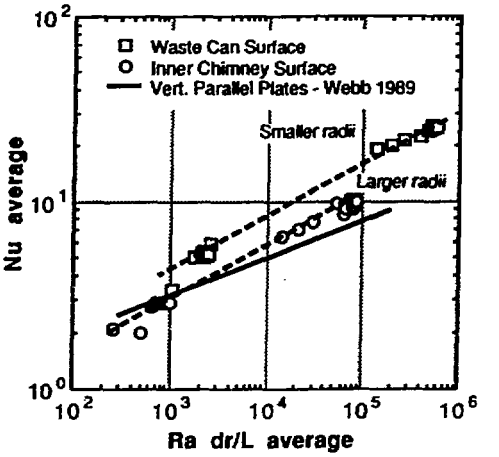

Figure 8: Average Nu number data for the inner channel.

area ratio is a technique which could be useful for analyzing other thermosyphon systems. The data is correlated as shown below for Re numbers ranging from 900 to 5,000.

$$Re_{inner} = 126\left(Ra\frac{\Delta r}{L}\right)^{0.27}_{avg}\frac{A_{outer}}{A_{inner}} \qquad (8)$$

Figure 10 shows the maximum can temperature as a function of total power released in the waste cans. The maximum wall temperature for the large diameter cans (small gap) is actually slightly less than the maximum temperature on the small diameter cans (large gap). As the radii of the waste can increases, the average heat flux off these surfaces de-

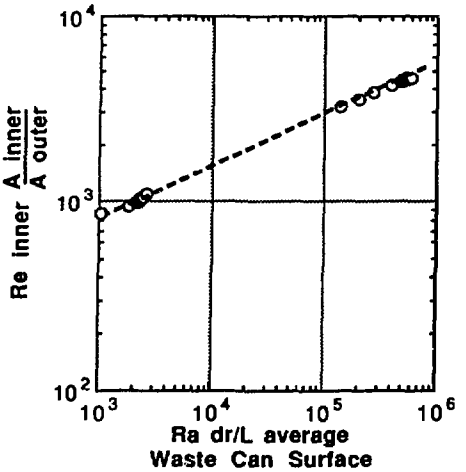

Figure 9: Correlation of Re number data with the average Ra number data from the waste can surface.

creases for a constant heat load. Decreasing the average flux works to decrease the maximum temperature. References [14] and [13] demonstrate that for $Ra\frac{\Delta r}{L} > 500$, the heat transfer off of each surface is independent of each other. If this was not true, decreasing the gap width would result in increased temepratures.

5 Conclusions

Experimental results are presented for the heat transfer within a thermosyphon. The apparatus has an inner channel and outer flow channel. The heat transfer in the inner channel is dominated by natural convection. The heat transfer in the outer channel is in the mixed convection regime. The general approach of the analysis is to base the empirical heat transfer correlations on the physics of the flow near the surface of interest.

The local Nu numbers for the large waste can surfaces compare well with previously conducted numerical work. The numerical work was for vertical parallel plates, with a constant heat flux on one surface, and the other surface thermally insulated. The average Nu numbers correlate well for the inner chimney and waste can surfaces. The average Nu numbers for the waste can surface are higher than those for the inner chimney surface because the radius of curvature is smaller. The trends shown by the experimental data are in good agreement with previously conducted experiments for parallel plates.

The same amount of total energy can be removed from the system for the large cans and the small cans.

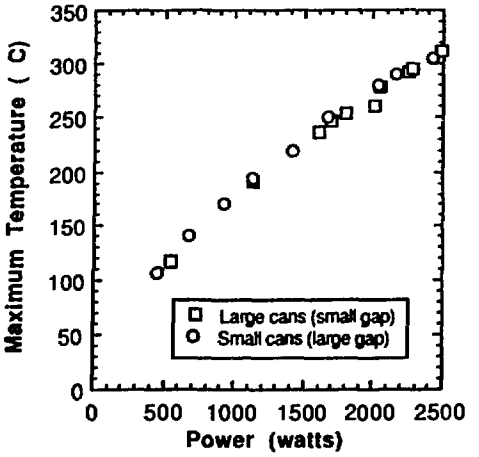

Figure 10: Maximum waste can temperatures for different power levels.

This is the result of the heat transfer off of the waste can surface being independent of the heat transfer off of the inner chimney surface for a sufficiently high average value of $Ra\frac{\Delta r}{L}$.

Acknowledgments

This work was supported by the U.S. Department of Energy, Nuclear Energy Programs, under contract no. W-31-109-ENG-38.

References

[1] Lin, T.-Y., and Hsieh, S.-S., "Natural Convection of Opposing/Assisting Flows in Vertical Channels with Asymmetrically Discrete Heated Ribs," *International Journal of Heat and Mass Transfer*, vol. 33, no. 10, pp. 2295-2309, 1990.

[2] Beine, B., Kaminski, V., and von Lensa, W., "Integrated Design of Prestressed Cast-Iron Pressure Vessel and Passive Heat Removal System for the Reactor Cell of a 200 MWth Modular Reactor," *Nuclear Engineering and Design*, vol. 136, pp. 135-141, 1992.

[3] Kwant, W., and Boardman, C.E., "PRISM-Liquid Metal Cooled Reactor Plant Design and Performance," *Nuclear Engineering and Design*, vol. 136, pp. 111-20, 1992.

[4] Mazria, E., The Passive Solar Energy Book, Rodale Press, Emmaus, PA, 1979.

[5] Chang, Y.I., "The Integral Fast Reactor," Nuclear Technology, vol. 88, November 1989, p.129-38.

[6] Mertol, A., and Greif, R., "A Review of Natural Circulation Loops," in *Natural Convection Fundamentals and Applications*, edited by Kakac, C., Aung, W., and Viskanta, R., Hemisphere Publishing Corporation, Washington, 1985.

[7] Gebhart, B., Jaluria, Y., Mahajan, R.L., and Sammakia, B., Buoyancy-Induced Flows and Transport, Hemisphere Publishing Corporation, Washington, D.C., 1988.

[8] Sparrow, E.M., and Gregg, J.L., 1956, "Laminar Free Convection From a Vertical Plate With Uniform Surface Heat Flux," *Transactions of the ASME*, February, p. 435-440.

[9] Fujii, T., and Fujii, M., 1976, "The dependence of Local Nusselt Number on Prandtl Number in the case of Free Convection Along a Vertical Surface with Uniform Heat Flux," *International Journal of Heat and Mass Transfer*, vol. 19, p. 121-22.

[10] Lee, H.R., Chen, T.S., and Armaly, B.F., 1988, "Natural Convection Along Slender Vertical Cylinders With Variable Surface Temperature," *Transactions of the ASME, Journal of Heat Transfer*, vol. 110, February, p. 103-108.

[11] Bodia, J.R., and Osterle, J.F., 1962, "The development of Free Convection Between Heated Vertical Plates," *Transactions of the ASME, Journal of Heat Transfer*, February, p. 40-4.

[12] Naylor, D., Floryan, J.M., and Tarasuk, J.D., 1991, "A Numerical Study of Developing Free Convection Between Isothermal Vertical Plates," *Transactions of the ASME, Journal of Heat Transfer*, vol. 113, August, p. 620-6.

[13] Miyatake, O., Fujii, T., Fujii, M., and Tanaka, H., "Natural Convective Heat Transfer Between Vertical Parallel Plates-One Plate With a Uniform Heat Flux and the Other Thermally Insulated," Heat Transfer-Japanese Research, vol. 4, 1973, pp.25-33.

[14] Aung, W., Fletcher, L.S., and Sernas, V., "Developing Laminar Free Convection Between Vertical Flat Plates with Asymmetric Heating," *International Journal of Heat and Mass Transfer*, vol. 15, pp. 2293-308, 1972.

[15] Bejan, A., 1984, Convection Heat Transfer, John Wiley and Sons, New York.

[16] Gau, C., Yih, K.A., and Aung, W., "Measurements of Heat Transfer and Flow Structure in Heated Vertical Channels," *Journal of Thermophysics and Heat Transfer*, vol. 6, no. 4, October-December 1992, p. 707-12.

[17] Hatton, A.P., and Quambry, A., "Heat Transfer in the Thermal Entry Length with Laminar Flow in an Annulus," *International Journal of Heat and Mass Transfer*, vol. 5, pp. 973-80, 1962.

[18] Webb, B.W., and Hill, D.P., "High Rayleigh Number Laminar Natural Convection in an Asymmetrically Heated Vertical Channel," *ASME Journal of Heat Transfer*, vol. 111, pp. 649-656, August 1989.

Nomenclature

A = *cross sectional area.*

Bo_x = $Ra_x Pr$

C_p = *specific heat.*

D_h = $\frac{4\,A_c}{P}$, *hydraulic diameter,* $2\Delta r$.

Gr = *Grashof number,* $\frac{Ra}{Pr}$.

h = *heat transfer coefficient.*

k = *thermal conductivity of fluid.*

$\dot{m}$ = *mass flowrate.*

Nu = *Nusselt number.*

P = *wetted perimeter.*

Pe_x = $Re_x Pr$.

q'' = *heat flux per unit area.*

Δr = $r_{outer} - r_{inner}$, *gap width.*

Ra = *Rayleigh number, see Equation* 6.

Ra_x = $\frac{q''_{loc} x^4 \beta\, g}{\alpha \nu k}$

Re = *Reynolds number, see Eqn.* 2.

Re_x = $\frac{\rho V x}{\mu} = \frac{\dot{m} x}{\mu A}$

T = *temperature.*

$x(i)$ *or* x = *axial location.*

β = *coefficient of volume expansion.*

ϵ = *surface emissivity.*

ρ = *density.*

μ = *absolute viscosity.*

ν = *kinematic viscosity.*